Inorganic Chemistry

Article

pubs.acs.org/IC

Chemical Implications of Incompatible Ligand versus Metal Coordination Geometry Preferences

Alice K. Hui,[†] Yaroslav Losovyj,[†] Richard L. Lord,*[,‡] and Kenneth G. Caulton*[,†]

[†]Indiana University, Department of Chemistry, 800 East Kirkwood Avenue, Bloomington, Indiana 47405, United States

[‡]Grand Valley State University, Department of Chemistry, 1 Campus Drive, Allendale, Michigan 49401, United States

Supporting Information

ABSTRACT: Binding an electron deficient pincer ligand which strongly dictates planar, *mer* stereochemistry, to a metal which prefers tetrahedral structure, e.g., d^{10} CuCl, is explored for possible intramolecular redox chemistry. Experiment shows that the pincer ligand 2,2′-bis-tetrazinyl pyridine, btzp, forms a complex (btzp)CuCl which is a chloride-bridged polymer in the solid state, hence with 20 valence electrons around copper. DFT calculations show that even the monomer has nonplanar copper with the tetrazinyl nitrogen lone pairs somewhat misdirected away from copper, with long Cu/N bonds, in a singlet ground state; 13.9 kcal/mol less stable is a triplet, whose electronic structure shows one electron from the ground state Cu(I) has been transferred to a pincer π^* orbital. Outer sphere electron transfer to (btzp)CuCl yields (btzp)Cu where the added electron has gone into the pincer, to leave a ligand-centered radical, characterized by EPR, chemical reactivity, and X-ray photoelectron spectroscopy.

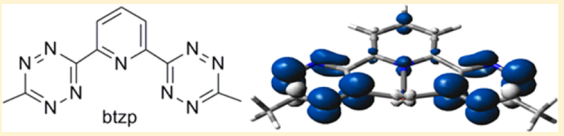

INTRODUCTION

Pincer ligands, which come in charge states 0, −1, and −2, are increasingly studied for their beneficial steric and electronic characteristics, involving donor atoms C, P, N, O, B, and Si.[1−4] These generally have a strong preference for meridional stereochemistry in binding a metal, but there is not much study of binding such pincers to a metal which is unsuitable for such *mer* stereochemistry. One principle holds that constraining a metal *away* from its electronically favored geometry results in *energetic* destabilization of the resulting structure, which can then be "harvested" as increased exothermic character in any reaction proceeding away from the "tense" or unstable geometry (*vide infra*). Reactant destabilization is a broadly useful principle for enhanced chemical reactivity: *cis* cyclooctyne, Dewar benzene, cubane, *cis*-azobenzene, norbornadiene/quadricyclane, constrained geometry olefin polymerization catalysts, etc. The challenge is thus to synthesize molecules incorporating this intrinsic instability. As an example, d^8 four coordinate complexes prefer a planar structure, fully compatible with a pincer *mer* constraint, while d^{10} complexes prefer a tetrahedral structure. Pincers are thus very common on d^8 complexes but rare on d^{10} metals.

We also wanted to marry this geometric destabilization to a second factor, redox noninnocence, via incorporation of a potentially redox-active donor functionality into the pincer. Nitrogen heterocycles $(CH)_{6-n}N_n$ built from sp^2 nitrogens (i.e., imines) are electrophiles,[5] in spite of the fact that coordination chemists think of them first as nucleophiles. This electrophilicity increases with increasing "*n*", because these nitrogens lower the energy of the π^* LUMO. Simple addition of electrons supports this idea, since Lewis structures immediately show (Scheme 1) the "storage" of 2 electrons at electronegative nitrogens, forming two amide functionalities (Lewis structures for a monoanion show one amide and a delocalized radical).

Scheme 1

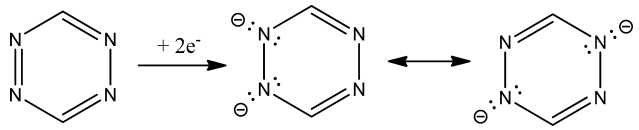

This reducibility is already evident in the surge of reports that bipyridyl and terpyridyl ligands are redox active, accepting electrons in preference to reduction at the metal.[6,7] When the heterocycle is attached to a cationic metal, this further facilitates reduction of the heterocycle, just as does quaternization of a heterocycle nitrogen with alkyl cations. Kaim[8−10] has been very active in showing that tetrazines can show redox activity when complexed to a variety of transition metals. We were interested in whether the heavy nitrogen content of 1,2,4,5-tetrazines[11] could lead these moieties to accept electrons from a reducing transition metal, and were attracted to a new pincer ligand (btzp, Scheme 2) incorporating *two* tetrazine arms.[12] We hoped to direct the coordinating power of a tetrazine toward a single

Scheme 2

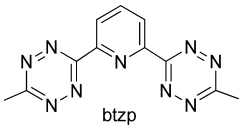

Received: November 19, 2013
Published: March 6, 2014

   dx.doi.org/10.1021/ic402866e | *Inorg. Chem.* 2014, 53, 3039−3047

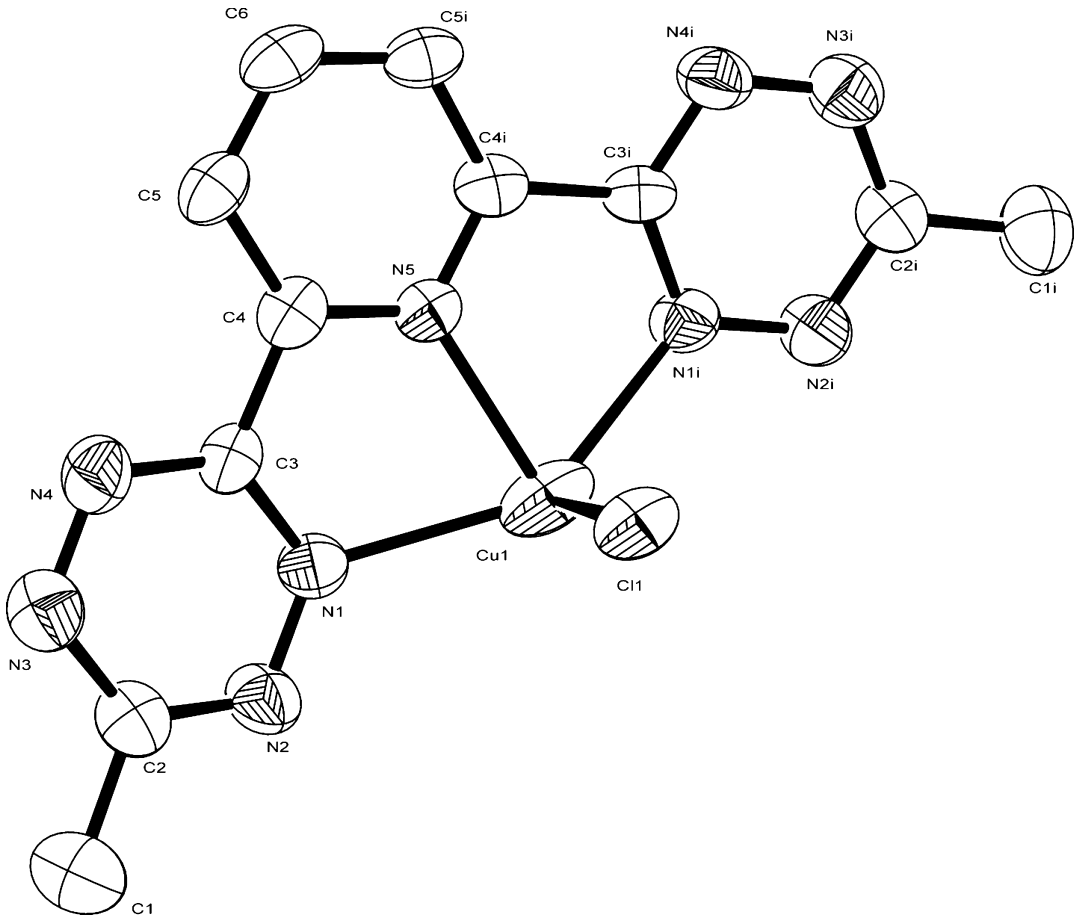

Figure 1. ORTEP drawing (50% probabilities) of the nonhydrogen atoms of the (btzp)CuCl repeat unit of the polymer chain. Cu, N5, and Cl1 lie on a crystallographic mirror plane. Selected structural parameters: Cu1−N5, 2.108(5) Å; Cu1−Cl1, 2.2851(16); Cu1−Cl1#1, 2.2887(15); Cu1−N1, 2.314(4); N1−N2, 1.333(6); N3−N4, 1.326(6); N5−Cu1−Cl1, 100.33(13)°; N5−Cu1−Cl1#1, 143.36(13); Cl1−Cu1−Cl1#1, 116.32(8); N5−Cu1−N1, 73.31(10); Cl1−Cu1−N1, 100.33(10); Cl1#1−Cu1-N1, 98.79(9); N1−Cu1−N1#2, 143.3(2); Cu1−Cl1−Cu1#3, 116.32(8).

metal, to avoid clusters or polymers, by employing pincer architecture. Will (btzp)CuCl exist as a structurally compromised Cu(I) complex, or will that destabilization built into this molecule lead btzp to oxidize Cu(I), and the resulting Cu(II) will then accept the *mer* ligand stereochemistry of the pincer radical anion? Alternatively, does the presence of two tetrazines in btzp enable outer sphere electron transfer to (btzp)CuCl, to form (btzp)Cu? Will this yield a complex of Cu(0) with a neutral btzp, or will it form a T-shaped 3-coordinate complex of copper(I), an energetically unfavorable structure for Cu(I), coordinated to radical anion $btzp^{-1}$? The outcome of combining these unusual geometric and electronic structural features is reported here.

RESULTS

Synthesis and Characterization of (btzp)CuCl. Reaction of equimolar CuCl with btzp in acetonitrile occurs in time of mixing to yield a deep red solution. If reacted in CD_3CN, the ^1H NMR spectrum of the solution shows new chemical shifts distinct from those of free btzp, but consistent with *equivalent* arms of the pincer ligand in a diamagnetic species. Curiously, the ESI(+) mass spectrum of a MeCN solution of this product shows the ion $Cu(btzp)_2^+$. However, at lower cone voltage, $Cu(btzp)(MeCN)^+$ is seen with strong intensity. This indicates chloride loss as a favored process for ion formation in MeCN and that 18 valence electron $Cu(btzp)(MeCN)^+$ cations are formed in the ionization chamber; however, no conclusion is warranted about solution phase speciation. Slow evaporation of the MeCN solvent yields red crystals which were shown by single crystal X-ray diffraction to be (btzp)CuCl (Figure 1), but with a structure which is a zigzag polymer of this repeat unit (Figure 2), bent at both copper and chloride. The species has a crystallographic mirror plane containing the Cu and Cl atoms of the zigzag chain. While this does not constrain the Cu/Cl distances to be equal, in fact the distances are not significantly different (2.2851(16) and 2.2887(15) Å). If the structure contained four coordinate 18 valence electron *monomers*, then this would compromise the coordination geometry at copper, since the planar pincer structure is incompatible with the tetrahedral preference of Cu(I). Surprisingly, the results show it is better for copper to adopt this 20 valence electron count environment, and avoid the unfavorable structure of a monomer. Copper in (btzp)CuCl is thus 5 coordinate, with an Addison parameter[13] of 0.45, hence half way between square pyramidal and trigonal bipyramidal. The misalignment of the pincer tetrazine rings is noteworthy, meaning that the nitrogen lone pairs are not well directed toward the metal, evident by the angles Cu/N/(para atom) being 171.7° for the pyridyl ring but 158.3° for the tetrazine ring (Figure 2). Tetrazine nitrogen to copper distances are long (2.314(4) Å), 0.2 Å longer than that to pyridine; the lengthening is a symptom of occupation of Cu/ligand σ^* orbitals for this 20 valence electron species. For

dx.doi.org/10.1021/ic402866e | *Inorg. Chem.* 2014, 53, 3039−3047

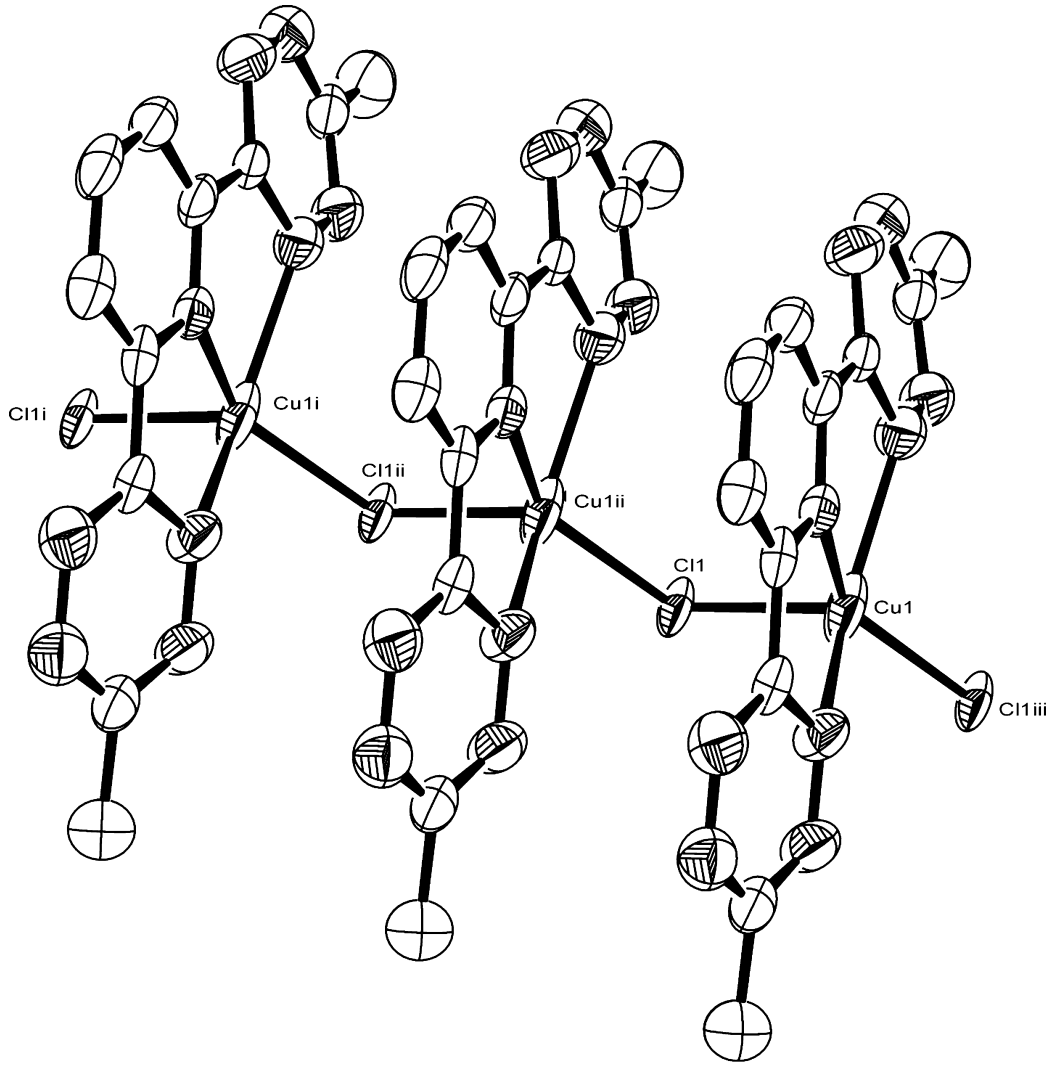

Figure 2. ORTEP drawing (50% probabilities) of the nonhydrogen atoms of the (btzp)CuCl polymer chain, showing three repeat units and one extra Cl. Shaded unlabeled atoms are nitrogen. Note the orientation of the tetrazine nitrogen lone pairs away from copper.

comparison, the Pt−N(arm) distances are only 0.1 Å longer than the Pt−N(center) distances in Pt^{II}(terpyridyl)X species.[14] Angles NCuCl involving pyridyl and the two chlorines are 100.33(13)° and 143.36(13)°, showing that the pincer is not accurately perpendicular to the polymer chain axis. It is also noteworthy that this molecule crystallizes from MeCN; hence, the nitrile is not competitive with bridging chloride for sites on copper in the solid state environment.

Btzp as Oxidant or Simply Lewis Base? What is the distribution of oxidation levels in (btzp)CuCl? Is it simply monovalent copper and neutral pincer, or does the pincer oxidize copper to Cu(II), forming radical anion $btzp^{-1}$; in the latter case, there are two possible spin states, singlet and triplet, but the observed NMR chemical shifts indicate the singlet state to be favored. Examination of the distances *within* the pincer ligand shows no significant (>3 esd's) differences from those in the free ligand;[12] hence, most consistent with this compound containing monovalent copper, the ligand does not oxidize Cu(I) here. Note also that coordination of copper to one tetrazine nitrogen does not significantly differentiate the tetrazine N/N distances (N1−N2, 1.333(6) Å; N3−N4, 1.326(6) Å in Figure 1), even though these are chemically inequivalent in the complex. The long Cu/N(tetrazine) bonds and N(tetrazine) lone pair misalignment may be symptomatic of Cu(I) being inherently too large to fit in the plane of the pincer; copper lies 0.3 Å above the plane of the pyridyl ring.

Why does this compound adopt a 20 valence electron structure; why does it polymerize, in the solid state, via chloride bridging? The 18 electron rule is based on the energy criterion of maximizing HOMO/LUMO gap (and to minimize the energy of the HOMO, using Walsh's rules[15] reasoning), but if structure is dictated by ligand constraints, that rule becomes secondary. This raises the question: how does "bad" monomer structure increase or create Lewis acidity at this metal? For example, does "bad" monomer structure lead to smaller HOMO/LUMO gap, and hence Lewis acidity? We turned to DFT calculations to test this hypothesis by evaluating the geometric and electronic structures of the unobserved monomeric (btzp)CuCl.

DFT Analysis of (btzp)CuCl Monomer. *Singlet.* We explored singlet and triplet species for the *monomer*. The DFT optimized structure for the singlet state fully (Figure 3, top right) confirms that the pincer constraints impose an unusual structure, and one which reflects some features also found in the repeat unit of the polymer. Cu/N distances to tetrazines are long at 2.30 Å, and both tetrazines have misaligned nitrogen

dx.doi.org/10.1021/ic402866e | *Inorg. Chem.* 2014, 53, 3039−3047

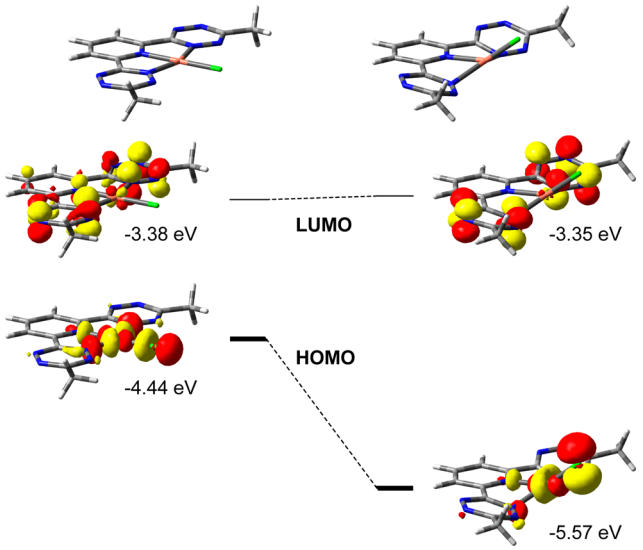

Figure 3. Plot showing HOMO/LUMO gap and orbital surfaces (iso = 0.05) from planar (left) to geometry-optimized singlet structures of (btzp)CuCl. Planar *geometry* is idealized to that of (btzp)$CuCl^+$, but orbitals are from full calculation of singlet (btzp)CuCl at that geometry.

lone pairs as evidenced by a dihedral angle of 14.2° between the pyridyl and tetrazine rings. The chloride ligand then lies out of the NNN plane, with a N(pyridyl)−Cu−Cl angle of 147.2° and an $N(tetrazine)_2Cu$ angle of 139.8°; these are both very similar to the angles in Figure 1. Multiple starting geometries for optimization all converged to this same structure, showing that this is not simply a local minimum. Minimization of a singlet beginning with either one or both tetrazine arms rotated away from bonding distance to copper again optimized to this same κ^3 geometry with two coordinated arms; this shows that these (long) bonds form spontaneously (i.e., with a favorable energy yield). For (btzp)CuCl, the HOMO/LUMO gap increases from 1.06 to 2.22 eV as the chloride bends out of plane (Figure 3). In this distortion, the LUMO energy changes little, consistent with its description as the in-phase combination of the tetrazine π^* orbitals (Figure 3); weak conjugation between the tetrazines via pyridine means this LUMO remains relatively unchanged when the bztp ligand becomes nonplanar in the freely optimized geometry of (btzp)CuCl. In contrast, the HOMO experiences significant stabilization (i.e., is less antibonding) due to the fact that the chloride lone pair overlaps less with the occupied $d_{x^2-y^2}$ in the nonplanar structure, in accord with Walsh's rule.[15] In summary, nonplanarity increases the HOMO/LUMO gap, a condition conventionally thought to enhance overall molecular stability.

Triplet. Especially informative is a study of the triplet state of monomeric (btzp)CuCl, for its dramatic differences from the singlet. The triplet is best described as a Cu^{II} complex of a monoreduced ligand radical anion; hence, this triplet is the result of intramolecular charge transfer with respect to the singlet ground state. The spin density map (Figure 4) clearly shows much spin on the ligand, with some also on copper and Cl. The minimum energy structure is fully *planar*, and the tetrazine nitrogens show a large (0.22 Å) shortening of Cu/N distances compared to the singlet structure, apparently consistent with *this* copper being content with planar geometry and having an $x^2 - y^2$ orbital (now singly occupied) more accepting of nitrogen lone pairs. Structure and oxidation state both indicate a conventional d^9 planar structure for copper. The CuCl distance is almost unchanged from that in the singlet state, which is unusual since electrostatics predicts shortening, but a trans influence causes it to elongate when Cl is trans to N(pyridyl); these two effects apparently cancel one another. As shown in Figure 4, the SOMOs of the triplet are very similar to the HOMO and LUMO, respectively, of the planar singlet (Figure 3), which is also consistent with calling this excited state the result of MLCT. One SOMO is $\sigma^*_{Cu/NandCl}$, and the other one is π^* on nitrogens. The triplet lies 13.9 kcal/mol above the singlet, in agreement with experiment that the ligand

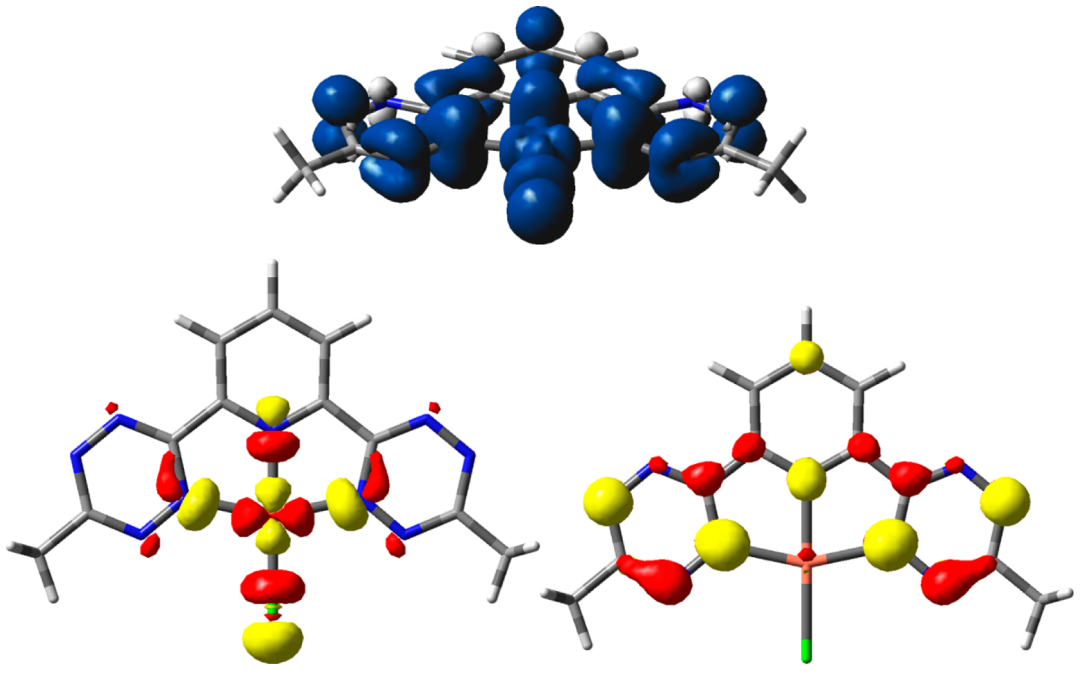

Figure 4. Isosurface plots of the spin density (iso = 0.002, top) and SOMOs (iso = 0.05, bottom) for the triplet (MLCT) state of (btzp)CuCl.

dx.doi.org/10.1021/ic402866e | *Inorg. Chem.* 2014, 53, 3039−3047

is unable to fully oxidize monovalent copper in the reaction of btzp with CuCl; (btzp)CuCl is therefore a ground state singlet, and the triplet is an excited state with metal-to-ligand charge transfer character. This charge transfer character of the excited state has been deduced, on the basis of optical studies, even for 2,2′-bipyridyl complexes of Cu(I).[14,16,17] All computational attempts to locate an antiferromagnetically coupled singlet metal-to-ligand charge transfer analogue ("open shell singlet") of this triplet reverted to the closed shell singlet electronic structure during the geometry optimization.

Nonpincer Analogue. We evaluated the impact of steric constraints of the pincer *connectivity* by DFT geometry optimization of the structure of Cu(pyridine)(3-methyl tetrazine)$_2$Cl. This minimized (Figure 5) to a distorted tetrahedral geometry, with all six angles 111 ± 9°. The N/Cu/N angles are large (112−120°), while the Cl/Cu/N angles are smaller (102−106°); this 3-fold distortion toward trigonal pyramidal Cu is apparently associated with a very long Cu/Cl bond length of 2.40 Å. The Cu−N tetrazine distance is 0.03 Å *shorter* than that to pyridine, at 2.07 Å, hence 0.24 Å shorter than calculated in the pincer singlet species; the tetrazine nitrogen lone pairs point accurately at copper, in contrast to the pincer case. Both of these criteria indicate that pincer constraints and coordination number 5 are the cause of long Cu/tetrazine distances in solid (btzp)CuCl. It is noteworthy that the HOMO/LUMO gap is not altered much (changed by 0.12 eV) from pincer to monodentate complex, but the change does stabilize the LUMO by 0.15 eV. Thus, it appears unproductive to try to attribute Lewis acidity to the HOMO/LUMO gap, particularly since the LUMO here is not metal-centered, but at the tetrazines; however, this does suggest that outer sphere reduction (i.e., electron transfer) would occur to the ligand.

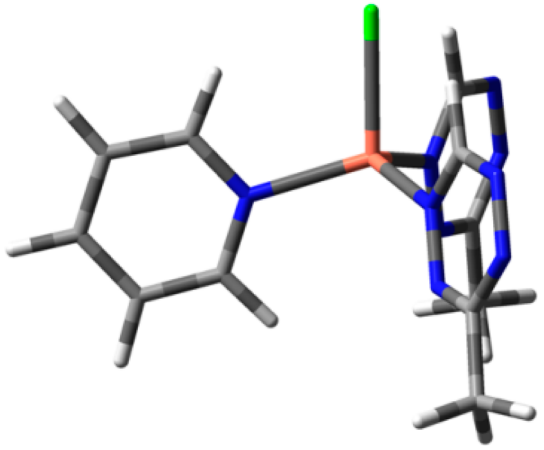

Figure 5. DFT minimum energy structure for Cu(pyridine)(3-methyl tetrazine)$_2$Cl, illustrating flattening of the CuN_3 unit from an ideal tetrahedron. Copper is pink, nitrogen is blue, and chlorine is green.

Redox Activity of (btzp)CuCl. Cyclic voltammetry of (btzp)CuCl in MeCN shows a reversible process with $E_{1/2}$ of 0.55 V (vs Ag/AgCl, Figure 6 a,b). Since the open circuit potential is measured as 0.04 V, this process is assigned to be an oxidation of the dissolved complex, and produces (btzp)CuCl$^+$. Using DFT, we also optimized the oxidized version of this species, whose orbitals are best described as $[Cu^{II}(bztp)^0Cl]^+$, and found it to be perfectly planar (Cu−Cl = 2.167 Å, Cu−N(pyr) = 2.019 Å, Cu−N(tet) = 2.136 Å) as expected for a complex containing a d^9 ion. This one electron oxidation of (btzp)CuCl decreases repulsions of the occupied d orbital with ligand nitrogen lone pairs, leading to shorter Cu/N distances.

In addition to this reversible oxidation, a reductive process is observed on scanning out to −0.6 V, an irrreversible one with $E_{pa} \sim -0.1$ V and $E_{pc} \sim --0.4$ V (Figure 6a); this is a much less negative potential for reduction than that of free btzp,[12] and we assign it to reduction of the ligand, facilitated by its attachment to cationic copper. There is no known zerovalent copper species, so reduction at metal is an unlikely assignment for this process. The smaller current flow on reduction is attributed to possible consumption of (btzp)CuCl arriving at the electrode, by free chloride liberated by previously reduced species; in addition, the insolubility of the reduction product (see below) removes it from reoxidation, as well as risking deposition on the electrode.

Chemical Reduction of (btzp)CuCl. *a. Synthesis and Reactivity.* Zerovalent copper is unknown in molecular species, and even in metal clusters. Reacting an acetonitrile solution of (btzp)CuCl with equimolar Cp_2Co immediately deposits a black solid for which we have found no satisfactory solvent. This black solid can be separated from any residual Cp_2Co and $[Cp_2Co]Cl$ by washing with acetonitrile. The black solid,

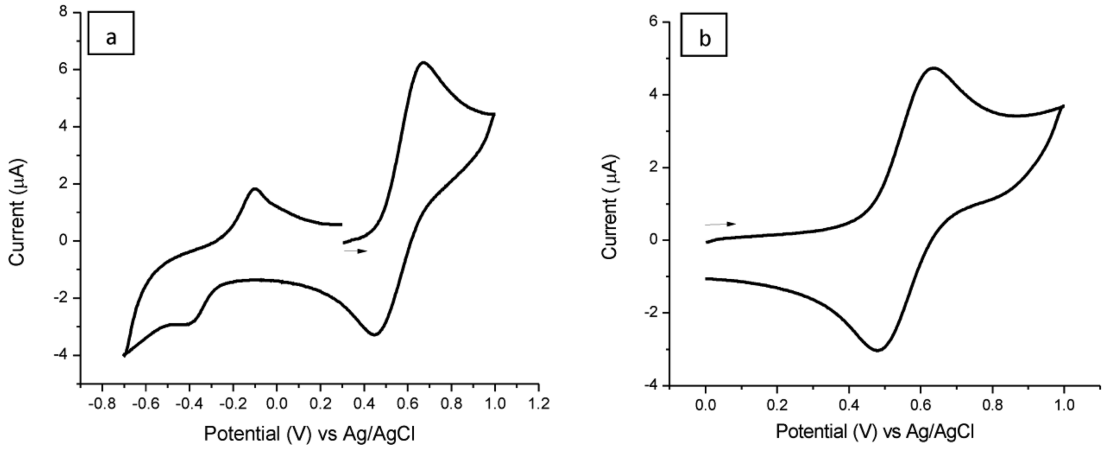

Figure 6. (a) Wide potential range (vs Ag/AgCl) cyclic voltammogram of (btzp)CuCl. (b) CV of the oxidative wave of (btzp)CuCl. Analyte concentration: 1.0 × 10^{-3} M in MeCN; 0.1 M in $[Bu_4N][PF_6]$ and 250 mV/s.

dx.doi.org/10.1021/ic402866e | Inorg. Chem. 2014, 53, 3039−3047

designated (btzp)Cu, when treated with CCl_4 (1:4 mol ratio) in acetonitrile dissolves immediately with reaction to form red (btzp)CuCl, identified by its ^{1}H NMR spectrum. This shows that the black solid reduction product does not contain degraded btzp, and that halogenation does not attack btzp in (btzp)Cu.

b. EPR Characterization. A solid state EPR spectrum (Figure 7) of a slurry of this (btzp)Cu shows a strong signal

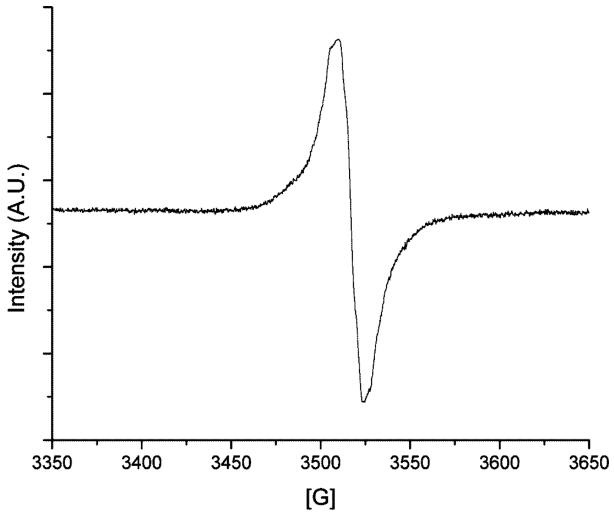

Figure 7. X-band EPR spectrum of solid (btzp)Cu suspended in MeCN. Experimental parameters: microwave frequency, 9.215 GHz; 100 kHz field modulation amplitude, 5 G; time constant, 300 ms, scan time, 2 min.

with g = 2.0042 which shows poorly resolved hyperfine structure. The spectrum in Figure 7 also indicates the small range of the three g values, which is characteristic of an organic radical and uncharacteristic of the spin−orbit coupling of copper, which makes Δg easily resolved. The spectrum can be simulated satisfactorily (see Supporting Information) with coupling to *four* ring nitrogens with a value of A_N = 4.6 G, which is typical of that in simple tetrazinyl radical anions.[12] This A value is too small, and the lines too numerous, to be due to copper hyperfine coupling, and so it is most consistent with a btzp^{-1} radical attached to Cu(I).

c. X-ray Photoelectron Spectroscopic Characterization. X-ray photoelectron spectroscopy (XPS) determines the ionization energy of core electrons of atoms in a molecule; core electrons report on their immediate environment, and are thus atom-specific.[18−20] Since that binding energy is sensitive to chemical environment, and especially atom oxidation state, XPS has substantial potential for the field of redox noninnocence, where location of valence electrons on constituent atoms differentiates alternative electronic structures. Because XPS signals are available for essentially all elements in the periodic table, the technique offers multiple perspectives on a single sample, which allows tests of internal consistency of oxidation state assignments. In the case at hand, XPS is useful in comparing (btzp)CuCl to its reduction product (btzp)Cu.

In contrast to the strong chloride XPS signal in (btzp)CuCl, the product of Cp_2Co reduction shows negligible chloride signal, confirming that reduction occurs with dehalogenation of the reagent copper complex. Both samples show (Figure 8) copper signals (Cu 2p) without the shakeup satellites characteristic of Cu(II), and the binding energy of the reduced

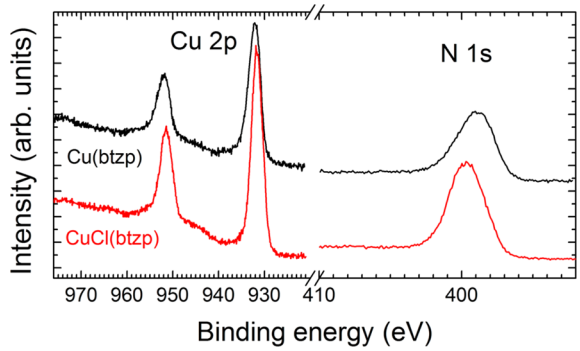

Figure 8. XPS spectra of (btzp)Cu (above) and (btzp)CuCl (below) recorded in the Cu 2p region and the N 1s region.

species (931.9 ± 0.15 eV) is clearly within experimental error identical to that (931.6 ± 0.15 eV) in unreduced (btzp)Cu^{I}Cl; this agreement is true of both the j = $^3/_2$ and j = $^1/_2$ copper peaks in Figure 8. The XPS in the nitrogen 1s region shows (Figure 8) only a single peak with no evidence of shoulders (i.e., no incipient resolution of inequivalent nitrogens), but the N 1s binding energy in (btzp)Cu is *lower* by 0.8 (±0.15) eV than that of (btzp)CuCl, consistent with charge buildup in the btzp ligand, with development of amide character at nitrogens. The SOMO of btzp^{-1} has spin density at all four nitrogens in a given tetrazine ring,[12] so this is why no single (anionic) nitrogen is resolved in the XPS spectrum. The overall conclusion is that reduction has occurred primarily in the btzp moiety in (btzp)Cu, since copper remains monovalent as judged by its 2p binding energy.

DFT Calculation on Cu(btzp). DFT geometry optimization of Cu(bztp) converges to the κ^3-bound planar structure with a T-shaped geometry at copper (Figure 9). Copper thus

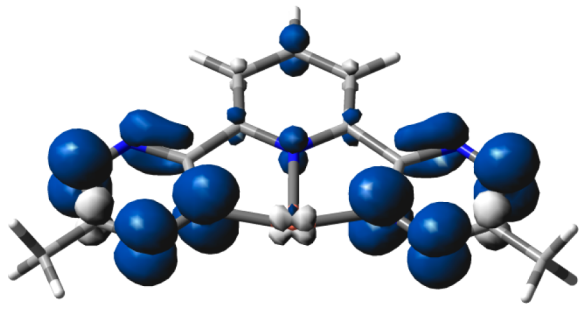

Figure 9. Spin density isosurface plot (0.002 au) of doublet Cu(bztp).

does fit in the btzp plane. The Cu−N_{pyr} and Cu−N_{tet} separations are short at 2.086 and 2.036 Å, respectively. Copper is essentially equidistant from both tetrazine nitrogens. This κ^3-bound Cu(bztp) adduct with a delocalized bztp^{-1} lies more than 40 kcal mol^{-1} below the other, charge-localized structures we found, clearly ruling out those others. The SOMO is π in character, being antisymmetric with respect to the molecular plane, and composed of π orbitals on the eight tetrazine nitrogens, with a small contribution from the pyridyl nitrogen and still smaller contribution from the copper dπ orbital. This is thus certainly not zerovalent copper, dominated by spin density in some sp hybrid orbital of the metal. Because of the C_{2v} symmetry, the spin density is located equally on both tetrazine rings. Apparently the reduction is thermodynamically easier when delocalized than if it were on only one tetrazine.

dx.doi.org/10.1021/ic402866e | *Inorg. Chem.* 2014, 53, 3039−3047

The spin density of Cu(btzp) (Figure 9) does show major population at the four nitrogens *nearest* the copper, so perhaps these are the four nitrogens whose hyperfine coupling we detect in our EPR spectrum. Alternatively, the broadening in our solid state EPR spectrum may conceal hyperfine coupling to the remaining nitrogens carrying spin density in Figure 9. Final resolution of this question requires a crystal structure determination, but we have not yet found a way to grow crystals.

DISCUSSION

Precedents to Planar Cu(I)? Most often, a planar tridentate ligand and Cu(I) in 1:1 mol ratio yield double helicates, $Cu_2L_2^{2+}$.[21−25] In these, each pincer arm binds κ^2 to one metal, and then donates the third arm to a second metal, in a complementary manner, in a clear effort to avoid a planar coordination geometry; as a result, the nitrogen donors are generally quasitetrahedral (or trigonal planar) around Cu(I).

Another relevant comparison compound is the d^{10} compound Zn(2,2′-terpyridyl)$_2^{2+}$ where the central pyridyl (2.068 Å) and the outer arm pyridyls (2.186 Å) have Zn/N bond lengths which differ by only 0.12 Å; the two pincer ligands are rigorously symmetry-related.[26]

Cu(I) with Coordination Number Greater than Four. A survey of the Cambridge Crystallographic Database for Cu(I) complexes with coordination number higher than four finds a limited number of examples, primarily with terpy and oligopyridines, as well as *ortho*-phenanthrolines, and all of these[21−25] show great (>0.5 Å) lengthening of Cu/N distances beyond the first four "normal" ones at ∼2.0 Å. None of these involve more than one electronegative nitrogen in the six-membered ring, so charge transfer (i.e., redox noninnocence) was not considered in those studies, and proximity at less than the sum of van der Waals radii was attributed to constraints of connectivity in the chelate backbone.

The chloride-bridged structure of (btzp)CuCl is thus unanticipated, although the long bonds to the two tetrazine arms are a symptom of the unusual, electron excessive character of the species. It is perhaps also a symptom of the fact that κ^2-btzp with one tetrazine rotated 90° from the pyridine plane may be energetically costly. That species might have been stabilized by intramolecular charge transfer from Cu^I to that rotated tetrazine (i.e., might have been a zwitterion), but our DFT work showed no support for that structure.

The present report shows an unusual structural compensation for Cu^I to an obligatory *planar* pincer ligand. Indeed, other reports, using more flexible and redox innocent pincer ligands attached to Cu^I and Ag^I, reveal that one arm either dangles free, leaving the pincer bidentate, or that arm binds to a second metal center, to give aggregated cluster species.[27−37]

Terpyridyl is another useful comparison standard to btzp in its interactions with Cu(I). It *also* shows symptoms of bad ligand adaptation to the preferred tetrahedral structure for d^{10}: a (terpy)CuI species[38] also has a five coordinate structure, also via bridging halide. Significantly, CuN distances there are all long, and the two CuN distances involving wingtip arm nitrogens are highly variable (by 0.15 Å), which is symptomatic of weak bonds; their average value is identical to the corresponding long distance in (btzp)CuCl, consistent with weak bonds of a 20 valence electron species. Many of these terpy structures reveal[21−25] the unsuitability of *mer* tridentate structure on Cu(I) by out-of-plane rotation of the arm pyridyls so that one pincer serves *two* copper centers. This appears to be a general principle. It is also true that the misdirection of tetrazine nitrogen lone pairs is diagnostic of weak bonds: considering only the monomer repeat unit (Figure 1), judging by bond angles ClCuN(py) and Cu(Ntetrazine)$_2$ at N5−Cu1−Cl1#1, 143.36(13)°, and N1−Cu1−N1#2, 143.3(2)°, that unit structure appears to be "reaching" for a nonplanar structure (i.e., location of copper orbitals) linked to tetrahedral parentage. Indeed, one referee commented that "the distortion might just as easily be described as copper(I) induced."

CONCLUSIONS

Although btzp is unable to oxidize CuCl here, the present work shows ready reduction by an external reductant into the btzp ligand in (btzp)CuCl, to give not bulk copper metal, but a ligated species (btzp)Cu, from which (btzp)CuCl can be recovered by halogen atom transfer. While (btzp)CuCl itself only has the redox product (btzp^{-1})Cu^{II}Cl as an excited state, it is clear that a more reducing metal might have a redox product as the ground state electronic structure. Product (btzp)Cu has a g value and nitrogen hyperfine coupling similar to those of [Cp_2Co](btzp),[12] all indicating that the added electron does not produce a zerovalent copper complex, but instead Cu^I complexed by btzp^{-1} radical anion; thus, its reaction with CCl_4 occurs by electron transfer from the ligand, without oxidation of copper. Finally, X-ray photoelectron spectroscopy appears to be a useful technique, especially for dealing with an insoluble compound like (btzp)Cu, and assay of the electronic environment of both copper and nitrogen in this solid strengthens the oxidation state conclusions from EPR spectroscopy and DFT orbital analysis.

EXPERIMENTAL SECTION

General. All manipulations were carried out under an atmosphere of ultrahigh purity nitrogen using standard Schlenk techniques or in a glovebox. Solvents were purchased from commercial sources, purified using Innovative Technology SPS-400 PureSolv solvent system or by distilling from conventional drying agents and degassed by the freeze−pump−thaw method twice prior to use. Glassware was oven-dried at 150 °C overnight and flame-dried prior to use. NMR spectra were recorded in various deuterated solvents at 25 °C on a Varian Inova-400 spectrometer (^{1}H: 400.11 MHz). Proton chemical shifts are reported in ppm versus solvent protic impurity, but referenced finally to $SiMe_4$. Mass spectrometry analyses were performed in an Agilent 6130 MSD (Agilent Technologies, Santa Clara, CA) quadrupole mass spectrometer equipped with a Multimode (ESI and APCI) source. All starting materials have been obtained from commercial sources and used as received without further purification. Cyclic voltammetry (CV) was carried out in a 3 mL conical electrochemical cell using a Princeton Applied Electronics potentiostat, model 263A. Electrolyte solution was prepared with 0.1 M tetrabutylammonium hexafluorophosphate ($TBAPF_6$) dissolved in high-performance liquid chromatography grade MeCN with 1 mM analyte concentrations. Argon, first passed through a vial of MeCN, was bubbled through the electrochemical cell to facilitate mixing, and the working electrode was cleaned after each scan. The electrodes used were composed of glassy carbon (working electrode), silver wire (reference electrode), and platinum wire (counter electrode).

The PHI Versa Probe II instrument equipped with monochromatic Al Kα source was used for XPS at base pressure ca. (4−8) × 10^{-10} Torr. The X-ray power of 65 W at 15 kV was used for all experiments with 260 μm beam size at take off angles of 45°. The instrument was calibrated to give a binding energy (BE) of 84.0 eV for Au $4f_{7/2}$ line as well as BEs of 284.8, 932.7, and 368.3 eV for the C 1s line of adventitious (aliphatic) carbon present on the nonsputtered samples, for Cu $2p_{3/2}$ and for Ag $3d_{5/2}$ photoemission lines, respectively. The ultimate Versa ProbeII instrumental resolution was determined to be

dx.doi.org/10.1021/ic402866e | Inorg. Chem. 2014, 53, 3039−3047

0.3 and 0.15 eV using the Fermi edge of the valence band for metallic silver for XPS and UPS (HeII line), respectively. The PHI dual charge compensation system was used on all samples. The electron charge neutralizer settings were adjusted for each sample to give a BE of 284.8 eV for the C 1s line. The high resolution spectra were taken with a minimum of 10−60 scans using a 0.05−0.1 eV step and 23 eV pass energy. All XPS spectra were recorded using PHI software *SmartSoft −XPS* v2.0 and processed using PHI *MultiPack* v9.0 and/or *CasaXPS* v.2.3.14. Peaks were fitted using a combination of Gaussian and Lorentzian line shapes with 30−50% of Lorentzian contents. Shirley background was used for curve-fitting. In general multiple spectra were recorded on different sample areas, to quantitatively evaluate reproducibility and avoid artifacts or detect radiation damage. The reduced species (btzp)Cu was handled and transferred under completely anaerobic conditions. The reduced sample shows trace impurity signal in the Co 2p region from the Cp_2Co reductant, and only small residual chloride impurity. The C 1s XPS signal does not show significant differences between (btzp)CuCl and (btzp)Cu, apparently because the charge buildup in btzp upon reduction occurs more at nitrogen; the LUMO of btzp, which is what becomes occupied upon reduction, has zero tetrazine carbon character, consistent with the insensitivity of the carbon XPS to reduction.

(btzp)CuCl. Ligand btzp (6 mg, 22.45 μmol) was dissolved in 5 mL of MeCN, and added to a stirred slurry of CuCl (2.44 mg, 24.70 μmol) and 5 mL of MeCN. The mixture was stirred for 10 min, and then filtered with a medium glass frit. The solvent was removed in vacuum to reveal a dark red solid; amorphous films of this solid appear black. Red needles were grown from slow evaporation in MeCN. The compound is insoluble in alkanes, benzene, fluorobenzene, toluene, and barely colors CH_2Cl_2 and THF, but is soluble in acetonitrile. ^{1}H NMR (400 MHz, MeCN): 3.10 (s, 6H), 8.48 (t, 1H, C−H Ar), 8.98 (d, 2H, C−H Ar). ESI(+) mass spectrum (MeCN solution): obsd 371.0532, calcd 371.0542 for (btzp)Cu(MeCN)$^+$ ($C_{13}H_{12}N_{10}{}^{63}Cu$); obsd 597.1276, calcd 597.1258 for $(btzp)_2Cu^+$ ($C_{22}H_{18}N_{18}{}^{63}Cu$). Scanning the cyclic voltammogram to more negative potentials, out to −1.2 V, there is an irreversible process (not shown in Figure 6a) beginning at about −0.6 V. Once this irreversible process has been scanned, a *new* additional peak is observed at −0.05 V, which we assign to oxidation of a product of the irreversible second reductive process, hence an artifact and not a property of (btzp)CuCl itself. It is therefore not shown in Figure 6.

Synthesis of (btzp)Cu and Its Oxidation by CCl_4. Equimolar Cp_2Co (2.57 mg, 13.65 μmol) was added to a stirring solution of (btzp)CuCl (5.00 mg, 13.65 μmol) in 10 mL of MeCN. Brown, near black precipitate of (btzp)Cu formed immediately upon addition, and the mother liquor was a pale yellow color. The mother liquor was removed with a disposable pipet (^{1}H NMR analysis showed this to contain Cp_2Co^+), and the precipitate was washed with copious amounts of MeCN until the solution layer was colorless. A slurry of the black precipitate and residual wash solvent was transferred to a Schlenk flask. This solid was used for EPR characterization. For reactivity testing, the dried solid was slurried in CD_3CN, and 5.29 μL (54.61 μmol) of CCl_4 was added. Upon stirring, the precipitate dissolved within minutes, and the solution became a dark red color. After 5 min, the product was shown to be identical with (btzp)CuCl by comparison of ^{1}H NMR data with an authentic sample.

Lewis Acidity of (btzp)CuCl. Reaction of a slurry of (btzp)CuCl in CD_2Cl_2 with $[N(n\text{-}Bu)_4]Cl$ (1:1 mol ratio) causes immediate dissolution of all solid, but gives a pink solution (color of free btzp), and ^{1}H NMR establishes that this is indeed free ligand, so apparently chloride displaces pincer, to also generate $[N(n\text{-}Bu)_4]CuCl_2$. These thermodynamic preferences are apparently ruled by the "compromising" geometry of the pincer being inferior to a simple chlorocuprate salt, so chloride is not a suitable Lewis base probe. Similar treatment with CO (1 atm) causes prompt dissolution of solid (btzp)CuCl slurried in CD_2Cl_2 to produce a dark red solution whose ^{1}H NMR spectrum shows three signals for btzp with chemical shifts indicating that the ligand is still attached to copper. This is noteworthy regarding Lewis acidity of (btzp)CuCl since the poor π basicity of Cu(I) causes CO to be only weakly bound to most copper complexes. This solution actively effervesces from loss of coordinated CO when head space pressure is decreased, showing poor binding of CO to copper. We were unable to obtain the infrared spectrum of this solution due to rapid CO loss during sampling.

COMPUTATIONAL DETAILS

Electronic structure calculations were carried out using DFT[39] as implemented in Gaussian09.[40] Geometry optimizations were performed at the B3LYP/LANL2DZ/6-31G(d,p)[41−47] level of theory with no symmetry constraints. All optimized structures were confirmed to have stable wave functions,[48,49] and then local minima by analyzing the harmonic frequencies.[50,51] Cartesian coordinates, frequencies, and energies for all optimized species may be found in Supporting Information.

ASSOCIATED CONTENT

Supporting Information

Full crystallographic details (including CIF format), additional spectroscopic data, and full DFT results. This material is available free of charge via the Internet at http://pubs.acs.org.

AUTHOR INFORMATION

Corresponding Author

*E-mail: caulton@indiana.edu. Phone: 812-855-4798.

Notes

The authors declare no competing financial interest.

ACKNOWLEDGMENTS

This work was supported in part by the IU Office of Vice President for Research. R.L.L. acknowledges support from GVSU start-up funds and a GVSU-CSCE Faculty Research Grant-in-Aid. Computational resources were provided by the Wayne State Grid.

REFERENCES

(1) Ozerov, O. V.; Guo, C.; Fan, L.; Foxman, B. M. *Organometallics* **2004**, *23*, 5573−5580.
(2) Schneider, S.; Meiners, J.; Askevold, B. *Eur. J. Inorg. Chem.* **2012**, *2012*, 412−429.
(3) Van Koten, G. *J. Organomet. Chem.* **2013**, *730*, 156−164.
(4) Weng, W.; Guo, C.; Moura, C.; Yang, L.; Foxman, B. M.; Ozerov, O. V. *Organometallics* **2005**, *24*, 3487−3499.
(5) Caulton, K. G. *Eur. J. Inorg. Chem.* **2012**, *2012*, 435−443.
(6) Bowman, A. C.; England, J.; Sproules, S.; Weyhermuller, T.; Wieghardt, K. *Inorg. Chem.* **2013**, *52*, 2242−2256.
(7) Scarborough, C. C.; Lancaster, K. M.; DeBeer, S.; Weyhermueller, T.; Sproules, S.; Wieghardt, K. *Inorg. Chem.* **2012**, *51*, 3718−3732.
(8) Kaim, W. *Coord. Chem. Rev.* **2002**, *230*, 127−139.
(9) Kavakli, C.; Gabrielsson, A.; Sieger, M.; Schwederski, B.; Niemeyer, M.; Kaim, W. *J. Organomet. Chem.* **2007**, *692*, 3151−3155.
(10) Sarkar, B.; Frantz, S.; Kaim, W.; Duboc, C. *Dalton Trans.* **2004**, *21*, 3727−3731.
(11) Clavier, G.; Audebert, P. *Chem. Rev.* **2010**, *110*, 3299−3314.
(12) Benson, C. R.; Hui, A. K.; Parimal, K.; Cook, B. J.; Chen, C.-H.; Lord, R. L.; Flood, A. H.; Caulton, K. G. *Dalton Trans.* DOI: 10.1039/C4DT00341A.
(13) Addison, A. W.; Rao, T. N.; Reedijk, J.; Van Rijn, J.; Verschoor, G. C. *J. Chem. Soc., Dalton Trans.* **1984**, 1349−1356.
(14) McGuire, R., Jr.; McGuire, M. C.; McMillin, D. R. *Coord. Chem. Rev.* **2010**, *254*, 2574−2583.
(15) Albright, T. A.; Burdett, J. K.; Whangbo, M.-H. *Orbital Interactions in Chemistry*, 1st Ed.; Wiley-Interscience: New York, 1984.
(16) Ruthkosky, M.; Kelly, C. A.; Castellano, F. N.; Meyer, G. J. *Coord. Chem. Rev.* **1998**, *171*, 309−322.

(17) McMillin, D. R.; Kirchhoff, J. R.; Goodwin, K. V. *Coord. Chem. Rev.* **1985**, *64*, 83−92.
(18) Fadley, C. S. *J. Electron Spectrosc. Relat. Phenom.* **2010**, *178−179*, 2−32.
(19) Hoang, T. K. A.; Webb, M. I.; Mai, H. V.; Hamaed, A.; Walsby, C. J.; Trudeau, M.; Antonelli, D. M. *J. Am. Chem. Soc.* **2010**, *132*, 11792−11798.
(20) Chusuei, C. C.; Brookshier, M. A.; Goodman, D. W. *Langmuir* **1999**, *15*, 2806−2808.
(21) Amendola, V.; Fabbrizzi, L.; Pallavicini, P. *Coord. Chem. Rev.* **2001**, *216−217*, 435−448.
(22) Constable, E. C.; Heirtzler, F.; Neuburger, M.; Zehnder, M. *J. Am. Chem. Soc.* **1997**, *119*, 5606−5617.
(23) Medlycott, E. A.; Hanan, G. S. *Chem. Commun.* **2007**, 4884−4886.
(24) Potts, K. T.; Keshavarz-K, M.; Tham, F. S.; Abruna, H. D.; Arana, C. *Inorg. Chem.* **1993**, *32*, 4450−4456.
(25) Potts, K. T.; Keshavarz-K, M.; Tham, F. S.; Abruna, H. D.; Arana, C. *Inorg. Chem.* **1993**, *32*, 4422−4435.
(26) Harvey, M. A.; Baggio, S.; Ibanez, A.; Baggio, R. *Acta Crystallogr., Sect. C* **2004**, *C60*, m375−m381.
(27) Al Thagfi, J.; Dastgir, S.; Lough, A. J.; Lavoie, G. G. *Organometallics* **2010**, *29*, 3133−3138.
(28) DeMott, J. C.; Basuli, F.; Kilgore, U. J.; Foxman, B. M.; Huffman, J. C.; Ozerov, O. V.; Mindiola, D. J. *Inorg. Chem.* **2007**, *46*, 6271.
(29) Harkins, S. B.; Peters, J. C. *J. Am. Chem. Soc.* **2004**, *126*, 2885−2893.
(30) Hayashi, A.; Okazaki, M.; Ozawa, F.; Tanaka, R. *Organometallics* **2007**, *26*, 5246−5249.
(31) Jurca, T.; Gorelsky, S. I.; Korobkov, I.; Richeson, D. S. *Dalton Trans.* **2011**, *40*, 4394−4396.
(32) Liu, X.; Pattacini, R.; Deglmann, P.; Braunstein, P. *Organometallics* **2011**, *30*, 3302−3310.
(33) Ma, G.; Ferguson, M. J.; McDonald, R.; Cavell, R. G. *Organometallics* **2010**, *29*, 4251−4264.
(34) Nielsen, D. J.; Cavell, K. J.; Skelton, B. W.; White, A. H. *Organometallics* **2006**, *25*, 4850−4856.
(35) Petrovic, D.; Bannenberg, T.; Randoll, S.; Jones, P. G.; Tamm, M. *Dalton Trans.* **2007**, *26*, 2812−2822.
(36) Rozenel, S. S.; Kerr, J. B.; Arnold, J. *Dalton Trans.* **2011**, *40*, 10397−10405.
(37) Zhou, Y.; Chen, W.; Wang, D. *Dalton Trans.* **2008**, 1444−1453.
(38) Feng, H.; Zhou, X.-P.; Wu, T.; Li, D.; Yin, Y.-G.; Ng, S. W. *Inorg. Chim. Acta* **2006**, *359*, 4027−4035.
(39) Parr, R. G.; Yang, W. *Density-Functional Theory of Atoms and Molecules*; Oxford University Press: New York, 1989.
(40) Frisch, M. J.; Trucks, G. W.; Schegel, H. B.; Scuseria, G. E.; Robb, M. A.; Cheeseman, J. R.; Scalmani, G.; Barone, V.; Mennucci, B.; Petersson, G. A.; Nakatsuji, H.; Caricato, M.; Li, X.; Hratchian, H. P.; Izmaylov, A. F.; Bloino, J.; Zheng, G.; Sonnenberg, J. L.; Hada, M.; Ehara, M.; Toyota, K.; Fukuda, R.; Hasegawa, J.; Ishida, M.; Nakajima, T.; Honda, Y.; Kitao, O.; Nakai, H.; Vreven, T.; Montgomery, J. A., Jr.; Peralta, J. E.; Ogliaro, F.; Bearpark, M.; Heyd, J. J.; Brothers, E.; Kudin, K. N.; Staroverov, V. N.; Keith, T.; Kobayashi, R.; Normand, J.; Raghavachari, K.; Rendell, A.; Burant, J. C.; Iyengar, S. S.; Tomasi, J.; Cossi, M.; Rega, N.; Millam, J. M.; Klene, M.; Knox, J. E.; Cross, J. B.; Bakken, V.; Adamo, C.; Jaramillo, J.; Gomperts, R.; Stratmann, R. E.; Yazyev, O.; Austin, A. J.; Cammi, R.; Pomelli, C.; Ochterski, J. W.; Martin, R. L.; Morokuma, K.; Zakrzewski, V. G.; Voth, G. A.; Salvador, P.; Dannenberg, J. J.; Dapprich, S.; Daniels, A. D.; Farkas, O.; Foresman, J. B.; Ortiz, J. V.; Cioslowski, J.; Fox, D. J. *Gaussian 09, Revision C.01*; Gaussian, Inc.: Wallingford, CT, 2010.
(41) Vosko, S. H.; Wilk, L.; Nusair, M. *Can. J. Phys.* **1980**, *58*, 1200−1211.
(42) Lee, C.; Yang, W.; Parr, R. G. *Phys. Rev. B* **1988**, *37*, 785−789.
(43) Becke, A. D. *J. Chem. Phys.* **1993**, *98*, 5648−5652.
(44) Stephens, P. J.; Devlin, F. J.; Chabalowski, C. F.; Frisch, M. J. *J. Chem. Phys.* **1994**, *98*, 11623−11627.
(45) Hay, P. J.; Wadt, W. R. *J. Chem. Phys.* **1985**, *82*, 270−284.
(46) Wadt, W. R.; Hay, P. J. *J. Chem. Phys.* **1985**, *82*, 284−299.
(47) Hay, P. J.; Wadt, W. R. *J. Chem. Phys.* **1985**, *82*, 299−311.
(48) Schlegel, H. B.; McDouall, J. J. In *Computational Advances in Organic Chemistry*; Oegretir, C., Csizmadia, I. G., Eds.; Kluwer Academic: Amsterdam, The Netherlands, 1991.
(49) Baurenschmitt, R.; Ahlrichs, R. *J. Chem. Phys.* **1996**, *104*, 9047−9053.
(50) Schlegel, H. B. *J. Comput. Chem.* **1982**, *3*, 214−218.
(51) Schlegel, H. B. *Wiley Interdiscip. Rev.: Comput. Mol. Sci.* **2011**, *1*, 790−809.